Initial condition for baryogenesis via neutrino oscillation

Takehiko Asaka,[1] Shintaro Eijima,[2] Hiroyuki Ishida,[3] Kosuke Minogawa,[4] and Tomoya Yoshii[4]

[1] *Department of Physics, Niigata University, Niigata 950-2181, Japan*

[2] *Institute of Physics, Laboratory for Particle Physics and Cosmology, École Polytechnique Fédérale de Lausanne, CH-1015 Lausanne, Switzerland*

[3] *Physics Division, National Center for Theoretical Sciences, Hsinchu, 30013 Taiwan*

[4] *Graduate School of Science and Technology, Niigata University, Niigata 950-2181, Japan*

(April 10, 2017)

arXiv:1704.02692v1 [hep-ph] 10 Apr 2017

Abstract

We consider a baryogenesis scenario via the oscillation of right-handed neutrinos with Majorana masses of the order of GeV, which are also responsible for neutrino masses by the seesaw mechanism. We study how the initial condition alters the prediction of the present baryon asymmetry by this mechanism. It is usually assumed that the abundance of right-handed neutrinos is zero after the reheating of the inflationary universe and they are produced in scattering processes by the renomalizable Yukawa interaction. However, the higher dimensional operator with right-handed neutrinos may provide an additional production which is most effective at the reheating epoch. It is shown that such an initial abundance of right-handed neutrinos can significantly modify the prediction when the strong washout of the asymmetry is absent. This leads that the parameter space of the model for the successful baryogenesis is enlarged.

1 Introduction

The baryon asymmetry of the universe (BAU) is one of the most mysterious numbers in particle physics and cosmology. The present baryon-to-entropy ratio, $Y_B = n_B/s$ with the baryon number density n_B and the entropy density s, is observed as [1]

$$Y_B^{\rm obs} = (8.677 \pm 0.054) \times 10^{-11} \,. \tag{1}$$

When the universe experiences the inflation, this asymmetry must be generated after the exponentially expanding period, more precisely, during or after the reheating process, which gives an initial condition of the hot big-bang universe. Such a mechanism, called as baryogenesis, requires three conditions [2]. Unfortunately, the Standard Model (SM) cannot satisfy some of these conditions. Especially, since the Higgs boson mass is measured as 125 GeV, the electroweak phase transition is a smooth cross-over (See, for example, the recent analysis [3] and references therein.) and then there is no way to lead a deviation from thermal equilibrium which is one of the above conditions. Thus, it is important to clarify new physics in order to explain the BAU between the inflation and the big-bang nucleosynthesis.

The baryogenesis scenarios with right-handed neutrinos are attractive since they can simultaneously account for tiny neutrino masses through the seesaw mechanism [4–10]. In the (canonical) leptogenesis scenario [11], the out-of-equilibrium decays of right-handed neutrinos can generate the lepton asymmetry which can be partially converted to the baryon asymmetry by the rapid sphaleron process for the temperatures $T > \mathcal{O}(10^2)$ GeV [12]. The observed value (1) can be explained when hierarchical right-handed neutrinos are heavier than $\mathcal{O}(10^9)$ GeV. (See, for example, Refs. [13–15].)

On the other hand, the flavor oscillation between right-handed neutrinos can also be responsible for the BAU [16, 17]. In this case the observed value (1) can be generated even when the Majorana masses are below the electroweak scale as long as the masses are quasi-degenerate. One of the attractive models which realizes this baryogenesis is the neutrino Minimal Standard Model (νMSM) [18,17]. In this scenario, two heavier ones among three right-handed neutrinos are responsible for baryogenesis and the remaining lightest one is a candidate of dark matter.

Since these right-handed neutrinos have tiny Yukawa coupling constants to realize the seesaw mechanism as well as to avoid the cosmological constraints on dark matter, the production rates by the scattering of the SM particles at the reheating epoch is negligible and then one can consider that there is essentially no right-handed neutrino in the beginning of the hot big-bang universe. However, unknown physics at high energy scale could produce right-handed neutrinos through the interactions suppressed by the cutoff scale of the model. One interesting possibility is the dimension-five interaction with right-handed neutrinos [19].

Although such an additional production is possible to affect the generation of the BAU, it has been shown in Ref. [19] that the effect is negligible if the dark matter abundance which is equally produced as the heavier ones does not overclose the universe. Here, we revisit this problem in several situations for the baryogenesis via neutrino oscillation. The important physical quantities for this scenario are the starting temperature of the right-handed neutrino oscillation $T_{\rm osc}$ which quantifies the oscillation effect

to baryogensis and the overall magnitude of the neutrino Yukawa coupling constants which quantifies the washout effect of the asymmetries. We will then consider several choices for these quantities leading to different situations of this baryogenesis.

As we will show below, when the neutrino Yukawa coupling constants are large enough, the initial abundance of the right-handed neutrinos does not affect on the produced BAU due to the strong washout effects. This result is consistent with the previous analysis. On the other hand, in the weak washout region, the situation is drastically changed and the impact on baryogenesis can be classified by $T_{\rm osc}$ and the initial condition of the matrices of densities. The off-diagonal element of the initial matrices of densities can significantly affect to the produced BAU when it is sufficiently large. As $T_{\rm osc}$ decreasing, the effects on the produced BAU from all elements of the initial matrices of densities are significant. This conclusion is different from the previous one.

This paper is organized as follows. We will present our framework in the next section. The impacts on the dark matter physics and baryogenesis will be discussed in Secs. 3 and 4. We will conclude our paper in Sec. 5. In addition, we review the production of right-handed neutrinos via higher dimensional operator in App. A and the parameterization of the neutrino Yukawa coupling constants in App. B. Finally, we present the evolution of the yield of the BAU in various situations in App. C.

2 The framework

We consider the νMSM, an extension of the SM by three right-handed neutrinos ν_{RI} ($I = 1,2,3$). The Lagrangian is given by

$$\mathscr{L}_{\nu\rm MSM} = \mathscr{L}_{\rm SM} + i\overline{\nu_{RI}}\gamma^\mu\partial_\mu\nu_{RI} - \left(F_{\alpha I}\,\overline{\ell_\alpha}\,\Phi\,\nu_{RI} + \frac{M_I}{2}\overline{\nu_{RI}^c}\,\nu_{RI} + H.c.\right), \tag{2}$$

where $\mathscr{L}_{\rm SM}$ is the SM Lagrangian, and Φ and ℓ_α ($\alpha = e,\mu,\tau$) are the weak doublets for Higgs and left-handed leptons, respectively. F is the matrix of Yukawa coupling constants and M_I is the Majorana mass of right-handed neutrino. Here and hereafter we shall work in the basis where the mass matrix of charged leptons and the Majorana mass matrix $M_M = {\rm diag}(M_1\,, M_2\,, M_3)$ are both diagonal.

We require the hierarchy between the Majorana mass M_I and the Dirac mass $[M_D]_{\alpha I} = F_{\alpha I}\langle\Phi\rangle$ ($\langle\Phi\rangle = 174$ GeV is the Higgs vacuum expectation value), $|[M_D]_{\alpha I}| \ll M_I$, to realize the seesaw mechanism. In this case, the mass eigenstates are active neutrinos ν_i ($i = 1,2,3$) and heavy neutral leptons (HNLs) N_I. The left-handed neutrino is then written as

$$\nu_{L\alpha} = U_{\alpha i}\,\nu_i + \Theta_{\alpha I}\,N_I^c\,, \tag{3}$$

where U is the PMNS mixing matrix for active neutrinos [20] and $\Theta = M_D/M_M$ is that for HNLs. The masses of active neutrinos m_i are determined from

$$[M_\nu]_{\alpha\beta} = -[M_D]_{\alpha I}[M_D]_{\beta I}M_I^{-1}\,, \quad U^\dagger M_\nu U^* = {\rm diag}(m_1\,,\, m_2\,,\, m_3)\,. \tag{4}$$

On the other hand, $N_I \simeq \nu_{RI}$ and the masses of HNLs are given by M_I.

In the νMSM, the lightest HNL N_1 is a candidate for dark matter and the heavier ones N_2 and N_3 realize the seesaw mechanism of active neutrino masses and baryogenesis via neutrino oscillation for the BAU. Since the dark matter can radiatively decay into pairs of active neutrino and photon, the mixing angle is highly constrained from X-ray observations depending on its mass [21]. According to such sever constraints, the dark matter abundance is difficult to be explained by the non-resonant production [22] together with the constraint from the structure formation [23]. On the other hand, the smaller mixing region is possible to explain the dark matter density by invoking the resonant production [24] in the presence of large lepton asymmetry at the production period. In any cases, since the Yukawa coupling constants of N_1 must be highly suppressed, it plays substantially no role for the seesaw mechanism and baryogenesis. As a result, the Yukawa coupling constants of $N_{2,3}$ should be chosen in order to explain the tiny active neutrino masses. (See App. B.) Thanks to the smallness of the Majorana masses, their coupling constants are found to be small.

The production of these right-handed neutrinos at high temperature region ($T \gg 10^2$ GeV) is ineffective as long as it is governed by the Yukawa interaction. This is because the required coupling constants are suppressed and the production rate being proportional to T is much slower than the expansion rate proportional to T^2. Consequently, it is considered that the abundance of right-handed neutrinos is essentially zero after the inflation. This is the initial condition for considering dark matter and baryogensis in the νMSM.

In this analysis we study the effects on physics of HNLs by a higher dimensional operator

$$\mathscr{L}_{\rm HD} = \frac{A_{IJ}}{2\Lambda}\Phi^\dagger\Phi\overline{\nu^c_{RI}}\nu_{RJ} + H.c., \tag{5}$$

where Λ is a cutoff scale and A is a coupling matrix. It should be noted that A is not a diagonal matrix in general, which is crucial for baryogenesis as will be shown later. We assume that all the elements A_{IJ} are of the same order of magnitude for simplicity. The impact of the operator (5) has already been discussed in Ref. [19], especially in the context of the Higgs inflation. Here, we revisit this problem paying a special attention to the impact on baryogenesis. In order to make a more general discussion we take the reheating temperature T_R as a free parameter without specifying the inflation model.

One of the impacts by the operator (5) is a correction to the Majorana masses for right-handed neutrinos

$$[\delta M_M]_{IJ} = -A_{IJ}\frac{\langle\Phi\rangle^2}{\Lambda} = -1.3\times10^{-5}\ {\rm eV}\, A_{IJ}\left(\frac{M_P}{\Lambda}\right), \tag{6}$$

where $M_P \simeq 2.4\times10^{18}$ GeV is the reduced Planck mass. It is seen that such corrections are significantly smaller than the masses of HNLs, namely much smaller than the typical mass $\mathscr{O}(10)$ keV of the sterile neutrino dark matter, and then they give only negligible impact on the masses of active neutrinos and HNLs. It should, however, be noted that such a correction might be important for the mass difference between N_2 and N_3, which is a key parameter for the baryogenesis via neutrino oscillation. In this case the mass difference used to estimate the BAU should be considered as the one given by $M_M + \delta M_M$.

Another consequence of the operator (5) is the additional production of right-handed neutrinos by scatterings of Higgs particles at the reheating epoch [19]. Note that the production rate due to the operator scales as T^3 and then a sizable amount of ν_R may be generated at the reheating epoch.

Let us consider the scattering process by the operator (5)

$$\phi_a + \phi_a \to \nu_{R_I} + \nu_{R_J}\,, \tag{7}$$

where four real scalar fields of Higgs doublet are denoted by ϕ_a ($a = 1,2,3,4$). We introduce the matrices of densities of the right-handed neutrino states with the positive and negative helicities

$$[\rho_N(\vec{k})]_{IJ} = \frac{1}{V}\mathrm{Tr}\left[\,\hat{\rho}(t)\,\hat{a}_J^\dagger(\vec{k},+)\,\hat{a}_I(\vec{k},+)\,\right], \quad [\rho_{\overline{N}}(\vec{k})]_{IJ} = \frac{1}{V}\mathrm{Tr}\left[\,\hat{\rho}(t)\,\hat{a}_J^\dagger(\vec{k},-)\,\hat{a}_I(\vec{k},-)\,\right], \tag{8}$$

where V is the space volume and $\hat{\rho}(t)$ is the density matrix operator. The annihilation and creation operators of ν_{R_I} with helicity h and momentum $\vec{k}$ are denoted by $\hat{a}_I(\vec{k},h)$ and $\hat{a}_I^\dagger(\vec{k},h)$, respectively. As explained in App. A, the contributions from the production process (7) are estimated as

$$[r_N]_{IJ} = 9.4\times10^{-4}\frac{M_P\,T_R}{\Lambda^2}\left[A^\dagger A\right]_{IJ}, \quad [r_{\overline{N}}]_{IJ} = 9.4\times10^{-4}\frac{M_P\,T_R}{\Lambda^2}\left[A^T A^*\right]_{IJ}. \tag{9}$$

Here r_N and $r_{\overline{N}}$ are the matrices of densities for right-handed neutrinos which are normalized by the equilibrium distribution function $f^{\rm eq} = (e^{|\vec{k}|/T}+1)^{-1}$. Notice that we have neglected the masses of right-handed neutrinos since $T_R \gg M_I$.

The initial values of the matrices of densities after the reheating, $[r_N]^I$ and $[r_{\overline{N}}]^I$, are then given by Eq. (9). It should be noted that any asymmetry between ν_R and $\overline{\nu}_R$ is not generated at the leading order since $[r_{\overline{N}}]^I = ([r_N]^I)^*$ as shown in Eq. (9). From now on we shall discuss the impacts of such initial abundances on dark matter and baryogenesis by ν_R.

3 Impact on dark matter

Now let us study the first topic of this article, the impact of the operator (5) on dark matter physics. In the νMSM the lightest HNL N_1 is a dark matter candidate. In the conventional scenario N_1 is produced by the scattering processes through the weak interactions with the mixing $\Theta_{\alpha 1}$ [22], and the dominant production occurs at the temperature $T_* \sim 100$ MeV for $M_1 \sim$ keV. The present abundance of dark matter is given by [1]

$$\Omega_{\rm dm}h^2 = 0.1188 \pm 0.0010\,, \tag{10}$$

where $\Omega_{\rm dm}$ is the present density parameter of dark matter component and h is the present Hubble parameter in unit of 100 km/sec/Mpc. This abundance can be explained by requiring the mixing elements as [25]

$$\sum_\alpha |\Theta_{\alpha 1}|^2 \simeq 8\times10^{-8}\left(\frac{M_1}{1\ \mathrm{keV}}\right)^{-2}. \tag{11}$$

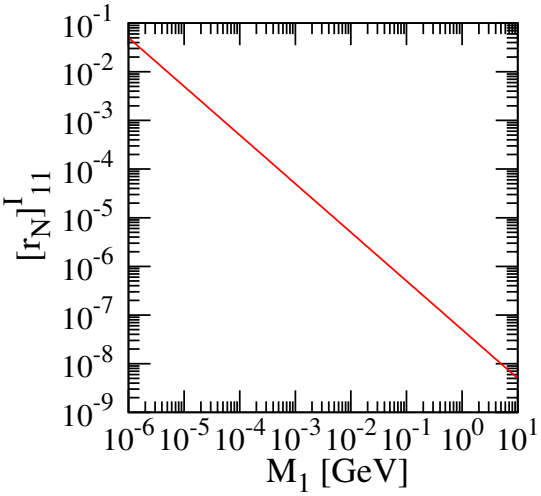

Figure 1: Initial value of $[r_N]^I_{11}$ required for the correct dark matter density $\Omega_{N_1} = \Omega_{\rm dm}$. The region above the red line is excluded because of the overclosure of the universe.

Such a dark matter candidate is constrained from various cosmological observations. From the cosmic X-ray observations, the radiative decay $N_1 \to \nu + \gamma$ is severely restricted and the strong upper bound on $\sum_\alpha |\Theta_{\alpha 1}|^2$ is obtained [21]. In addition, N_1 with keV mass, which plays a role of warm dark matter, receives the constraint from the cosmic structure and the lower bound on M_1 is obtained [23]. The present status of this dark matter scenario is difficult to realize within the simplest thermal history. See the discussion in Ref. [26, 27].

On the other hand, when there exists a sizable lepton asymmetry around $T \simeq T_*$, the resonant production of N_1 occurs [24]. In this case the mixing elements much smaller than Eq. (11) can account for the dark matter abundance (10) and the severe X-ray bound can be avoided. See the analysis in Ref. [28]. Interestingly, as shown in Refs. [29, 30], the required lepton asymmetry can be originated in the dynamics of N_2 and N_3 without introducing any new physics.

Now we turn to discuss the impact of the higher dimensional operator (5). As pointed out in Ref. [19], enough number of N_1 can be generated at the reheating epoch. We can estimate the density parameter of N_1 from the initial values of $[r_N]^I_{11}$ and $[r_{\overline{N}}]^I_{11}$ as

$$\Omega_{N_1} h^2 = 0.11 \left(\frac{\left([r_N]^I_{11} + [r_{\overline{N}}]^I_{11} \right)}{10^{-2}} \right) \left(\frac{M_1}{10\ {\rm keV}} \right) . \tag{12}$$

Note that $[r_N]^I_{11} = [r_{\overline{N}}]^I_{11}$. It is thus found that the initial value of $[r_N]^I_{11}$ must be

$$[r_N]^I_{11} < 5.6 \times 10^{-3} \left(\frac{10\ {\rm keV}}{M_1} \right) , \tag{13}$$

in order that the abundance Ω_{N_1} in Eq. (12) does not exceed the observed value (10), which is shown in Fig. 1. This bound can be translated into the upper bound on T_R, but it is a mild bound. For instance, when $\Lambda = M_P$, $A = \mathcal{O}(1)$, and $M_1 > \mathcal{O}(10^2)$ keV, the condition can be satisfied even if $T_R = M_P$. See Fig. 2.

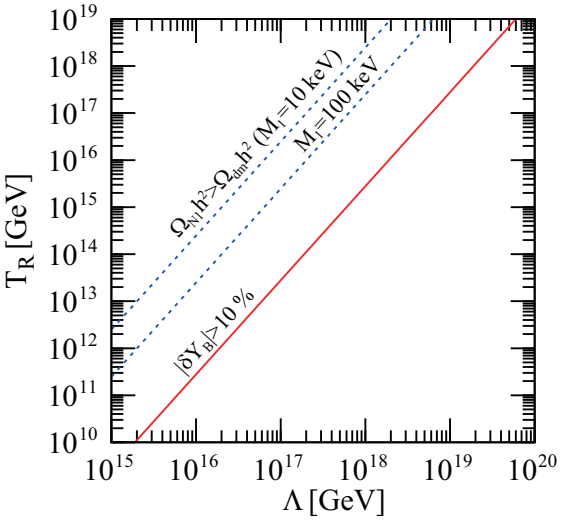

Figure 2: Upper bounds on the reheating temperature T_R in terms of the cutoff scale Λ. The bounds from the dark matter abundance $\Omega_{N_1}h^2 < \Omega_{\rm dm}h^2$ for M_1=10 keV and 100 keV are shown by the blue dashed lines. The bound from the BAU $|\delta Y_B| < 10$ % when $\Delta M = 10^{-13}$ GeV and $X_\omega = 1$ is also shown by the red solid line.

When the mixing of N_1 is smaller than the value (11) and the initial values of the matrices of densities take the value as shown in Fig. 1, the alternative scenario of dark matter is possible [19].[#1] For example, when $\Lambda = M_P$, $T_R = 10^{13}$ GeV, and $A = \mathcal{O}(1)$, N_1 with mass $M_1 = 4.9$ GeV becomes a viable candidate for dark matter. One might worry about the stability of such a heavy particle. It should be noted, however, that we can switch off the Yukawa coupling for N_1 (*i.e.*, $F_{\alpha 1}$=0) since the operator (5) is responsible for the production. In this case, the discrete symmetry Z_2 associated with N_1 arises, under which only $N_1 = \nu_{R1}$ changes as $N_1 \to -N_1$. This symmetry, in which the operator (5) is invariant, ensures the complete stability of N_1. On the other hand, the tests of such a dark matter candidate become difficult since the mixing of N_1 disappears. The test in the cosmic X-ray background [27] is impossible because $N_1 \to \nu\gamma$ is forbidden and the test at KATRIN [31,32] is also impossible because N_1 cannot be produced in tritium beta decay.

4 Impact on baryogenesis

Next, we turn to discuss the impact of the initial abundance (9) on baryogeneis. In the considering model, the sufficient amount of the BAU can be generated by the mechanism via neutrino oscillation, namely by the oscillation between the quasi-degenerate N_2 and N_3 [16, 17]. We then write $M_2 = M_N - \Delta M/2$ and $M_3 = M_N + \Delta M/2$ with $M_N \gg \Delta M$. Such a impact has also been studied in Ref. [19]. It has been shown that, when all the initial values of the matrices of densities are sufficiently small as shown in Eq. (13) in order to avoid the overproduction of dark matter particle, the yield of the BAU does not

[#1] It is possible to realize a mixed dark matter scenario where both N_1's produced at the reheating and $T \simeq$100 MeV periods contribute the present dark matter density comparably.

change significantly. We shall revisit this problem paying a special attention to the initial value of the off-diagonal element $[r_N]^I_{23}$. Such an element can be generated at the reheating epoch because the coupling matrix A is not diagonal in general and the basis of right-handed neutrinos at high temperature regions is different from the vacuum one. See the discussion in App. A. As we will show below, the initial value of $[r_N]^I_{IJ}$ can alter the final BAU significantly even if they satisfy the condition (13), which should be contrasted to the previous results in Ref. [19].

We estimate the yield of the BAU Y_B by solving the coupled equations for the matrices of densities $[\rho_N]$ and $[\rho_{\overline{N}}]$ for right-handed neutrinos with positive helicity and their anti-particles with negative helicity, respectively as well as chemical potentials for (left-handed) leptons. When the neutrino Yukawa coupling constants are sufficiently small, there are three conserved charges $X_\alpha = B/3 - L_\alpha$, where B is the baryon number and L_α is the lepton number of a specific flavor α. The chemical potential of X_α (which is divided by the temperature and is dimensionless) is denoted by μ_{X_α}, while the chemical potential of L_α is μ_α, and they satisfy

$$\mu_\alpha = -\sum_\beta C_{\alpha\beta}\,\mu_{X_\beta}\,, \tag{14}$$

where

$$C_{\alpha\beta} = \frac{1}{711}\begin{pmatrix} 221 & -16 & -16 \\ -16 & 221 & -16 \\ -16 & -16 & 221 \end{pmatrix}. \tag{15}$$

The equations for $[r_N]$, $[r_{\overline{N}}]$ and μ_{X_α} have been discussed in Refs. [16,17,29,30,33–43]. Here we shall follow the equations in Ref. [44]:

$$\frac{dr_N}{dt} = -i\left[\langle H\rangle,\, r_N\right] - \frac{\langle\gamma_N^{(0)}\rangle}{2}\left\{F^\dagger F,\, r_N - 1\right\} + \langle\gamma_N^{(1)}\rangle F^\dagger\mu F - \frac{\langle\gamma_N^{(2)}\rangle}{2}\left\{F^\dagger\mu F,\, r_N\right\}, \tag{16}$$

$$\frac{dr_{\overline{N}}}{dt} = -i\left[\langle H^*\rangle,\, r_{\overline{N}}\right] - \frac{\langle\gamma_N^{(0)}\rangle}{2}\left\{F^T F^*,\, r_{\overline{N}} - 1\right\} - \langle\gamma_N^{(1)}\rangle F^T\mu F^* + \frac{\langle\gamma_N^{(2)}\rangle}{2}\left\{F^T\mu F^*,\, r_{\overline{N}}\right\}, \tag{17}$$

$$\begin{aligned}\frac{d\mu_{X_\alpha}}{dt} = -\frac{9\zeta(3)}{\pi^2}\Bigg\{&\frac{\langle\gamma_N^{(0)}\rangle}{2}(Fr_NF^\dagger - F^* r_{\overline{N}}F^T)_{\alpha\alpha} \\ &+ \mu_\alpha\left[\frac{\langle\gamma_N^{(2)}\rangle}{2}(Fr_NF^\dagger + F^* r_{\overline{N}}F^T)_{\alpha\alpha} - \langle\gamma_N^{(1)}\rangle(FF^\dagger)_{\alpha\alpha}\right]\Bigg\},\end{aligned} \tag{18}$$

where

$$\langle H\rangle = \frac{M_N^2}{2k} + \frac{T^2}{8k}F^\dagger F, \quad k = \frac{18\zeta(3)}{\pi^2}\,T\,, \tag{19}$$

$$\langle\gamma_N^{(i)}\rangle = A_i\left[c^{(i)}_{LPM} + y_t^2 c_Q^{(i)} + (3g^2 + g'^2)\left(c_V^{(i)} + \log\left(\frac{1}{3g^2 + g'^2}\right)\right)\right], \tag{20}$$

$$A_0 = 2A_1 = -4A_2 \equiv \frac{4\pi^2}{3\zeta(3)}\frac{T}{3072\pi}, \tag{21}$$

and the values of constants are $(c_{LPM}^{(0)}, c_{LPM}^{(1)}, c_{LPM}^{(2)}) = (4.22, 3.56, 4.77)$[#2], $(c_Q^{(0)}, c_Q^{(1)}, c_Q^{(2)}) = (2.52, 3.10, 2.27)$, and $(c_V^{(0)}, c_V^{(1)}, c_V^{(2)}) = (3.17, 3.83, 2.89)$. In the above equations, we use the running coupling constants at the scale T evaluated from the one-loop renormalization group equations. We use the coupling constants at top mass scale as $y_t = 0.93690$, $g' = 0.35830$, $g = 0.64779$, and $g_3 = 1.1666$ [46].

We solve numerically the kinetic equations (16)–(18) and evaluate the chemical potential μ_{X_α} at $T = T_{\rm sph}$ where $T_{\rm sph}$ is the freeze-out temperature of the sphaleron process. In this analysis we take $T_{\rm sph} = 130$ GeV [47]. The prediction of the present BAU is then given by

$$Y_B = 1.3 \times 10^{-3} \sum_\alpha \mu_{B/3-L_\alpha}(T_{\rm sph}), \tag{22}$$

where we have assumed that there is no additional entropy production for $T < T_{\rm sph}$. The yield of the BAU depends on M_N, ΔM, and the neutrino Yukawa coupling constants. Especially, M_N and ΔM are important parameters to determine the temperature $T_{\rm osc}$ when their flavor oscillation starts, which is given by

$$T_{\rm osc} = \left(\frac{1}{6} M_0 \Delta M M_N\right)^{1/3} = 320\ {\rm GeV} \left(\frac{M_N}{3\ {\rm GeV}}\right)^{1/3} \left(\frac{\Delta M}{10^{-10}\ {\rm GeV}}\right)^{1/3}, \tag{23}$$

where $M_0 = 7.1 \times 10^{17}$ GeV. In addition, the parameter X_ω in the neutrino Yukawa coupling constants (see Eq. (39) in App. B) is another important parameter for baryogenesis. This is because it determines the overall scale of the Yukawa coupling constants (see, for example, the discussion in Ref. [48]), and then the yield of the BAU depends on it siginificantly.

Now we are at the position to show how the yield of the BAU depends on the initial value of the matrices of densities. We shall discuss the impact of each element separately and then consider the three cases in which we assume the non-zero initial value only for (i) $[r_N]^I_{22}$, (ii) ${\rm Re}[r_N]^I_{23}$, and (iii) ${\rm Im}[r_N]^I_{23}$. We should mention here that $[r_N]_{32}$ also has the initial value satisfying $r_N = r_N^\dagger$ for the cases (ii) and (iii). The impact of the initial value $[r_N]^I_{33}$ is similar to the case (i), namely the magnitude of the additional contribution is the same but the sign is opposite. We should note that the initial value for anti-neutrinos is taken as $[r_{\overline{N}}]^I_{IJ} = ([r_N]^I_{IJ})^*$ so that there is no asymmetry for any number initially.

The effect of the non-zero initial value is represented by the deviation which is defined by

$$\delta Y_B = \frac{Y_B|_{[r_N]^I_{IJ}\neq 0} - Y_B|_{[r_N]^I_{IJ}=0}}{Y_B|_{[r_N]^I_{IJ}=0}}. \tag{24}$$

Here $Y_B|_{[r_N]^I_{IJ}=0}$ is the yield of the BAU when all initial values are taken to be zero and $Y_B|_{[r_N]^I_{IJ}\neq 0}$ is the one when the inital value is present. We fix $M_N = 3$ GeV as a representative value and take the parameters of the Yukawa coupling constants explained in Apps. B and C. We then study how the deviation δY_B changes by the initial value of the matrices of densities.

First of all, let us consider the case when $X_\omega = 1$ and the Yukawa coupling constants are sufficiently small so that the washout effect is negligible. The results of the deviation (24) are represented in Fig. 3. In this case the impact of the initial values diverge depending on ΔM.

[#2] We use the values at $T = 10^4$ GeV for simplicity. See the detail in Ref. [45].

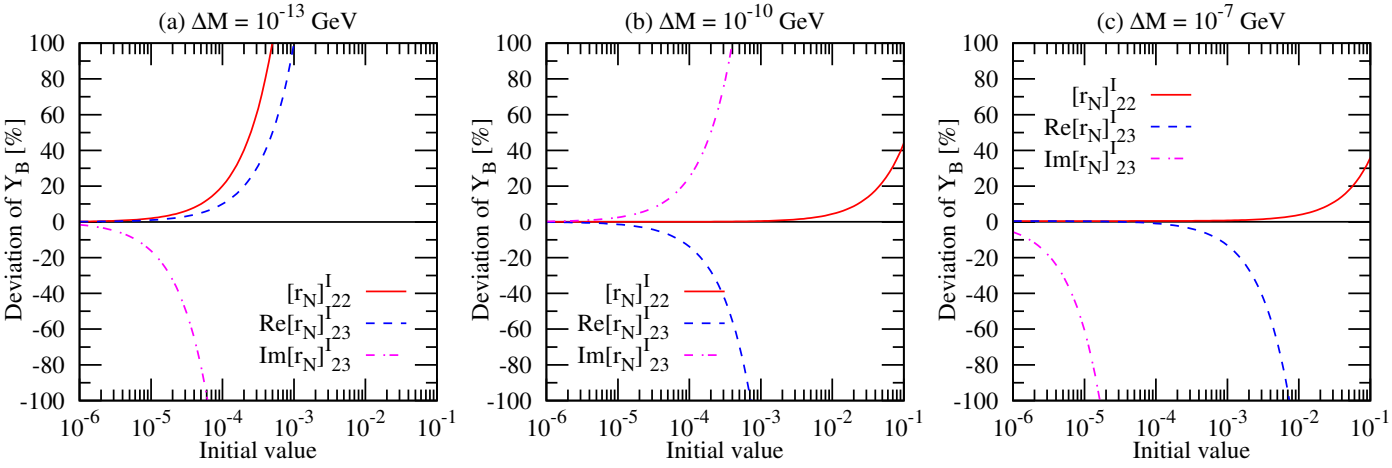

Figure 3: Deviation of the yield of the BAU in terms of the initial value of the non-zero element of the matrix of densities $[r_N]^I_{22}$ (red solid line), $\mathrm{Re}[r_N]^I_{23}$ (blue dashed line), and $\mathrm{Im}[r_N]^I_{23}$ (magenta dash dotted line). We fix $X_\omega = 1$ and take (a) $\Delta M = 10^{-13}$ GeV, (b) $\Delta M = 10^{-10}$ GeV, and (c) $\Delta M = 10^{-7}$ GeV.

For the region with $\Delta M \ll 10^{-10}$ GeV, the oscillation temperature $T_{\rm osc}$ (23) is much smaller than $T_{\rm sph}$ and the oscillation effect to generate the BAU is ineffective. In this case, as shown in Fig. 3 (a), the initial value of each element $[r_N]^I_{IJ}$ modifies significantly the prediction of the BAU. It is seen that the deviation of Y_B becomes larger than 10 % when the initial value is large than $\mathcal{O}(10^{-5})$ in each element. This critical value from the BAU is much smaller than $\mathcal{O}(10^{-2})$ which is needed to avoid the overclosure of the universe by N_1 with $M_1 \simeq 10$ keV given in Eq. (12). To make this point clearer, we also show in Fig. 2 the upper bound on T_R by requiring that the deviation of Y_B is sufficiently small as $|\delta Y_B| < 10$ %. It is found that the bound from δY_B is more stringent than that from the dark matter density if $M_1 < \mathcal{O}(10)$ MeV. The bound gives the condition for the inflation under which the present BAU can be predicted only by the weak scale physics. This clearly shows that the prediction of the baryon asymmetry can be affected by the processes at the reheating epoch even if one demands that such a effect on dark matter is negligible, which is opposite to the previous one [19].

We find that the key parameter in this case is $\mathrm{Im}[r_N]_{23}$. Each initial value, as shown in Fig. 4, gives the additional contribution to $\mathrm{Im}[r_N]_{23}$ and, if it alters the value at $T = T_{\rm sph}$ in which the baryogenesis is most effective, the yield of the BAU is modified significantly. See also Fig. 7 in App. C.1.1.

Next, we consider the region $\Delta M = 10^{-10}$ GeV in which $T_{\rm osc} \sim T_{\rm sph}$. In fact, as shown in Ref. [17], this case gives the maximal value of the BAU as a function of ΔM (if one can neglect the washout effect). In this case, as shown in Fig. 3 (b), although the initial value of the diagonal element does not change the yield of the BAU as long as $[r_N]^I_{22} < \mathcal{O}(10^{-2})$, the off-diagonal elements, $\mathrm{Re}[r_N]^I_{23}$ and $\mathrm{Im}[r_N]^I_{23}$, change the prediction if they become larger than $\mathcal{O}(10^{-5})$. The behaviors associated with $[r_N]^I_{22}$ and $\mathrm{Re}[r_N]^I_{23}$ do not change much even for $\Delta M \gg 10^{-10}$ GeV and $T_{\rm osc} \gg T_{\rm sph}$, but the final BAU becomes more sensitive to $\mathrm{Im}[r_N]^I_{23}$. See Fig. 3 (c). Therefore, we have found that the initial values of the matrices of densities can change the prediction of the BAU drastically even if the overproduction of dark matter is avoided. Especially, the impact from the off-diagonal elements is found to be significant in any cases.

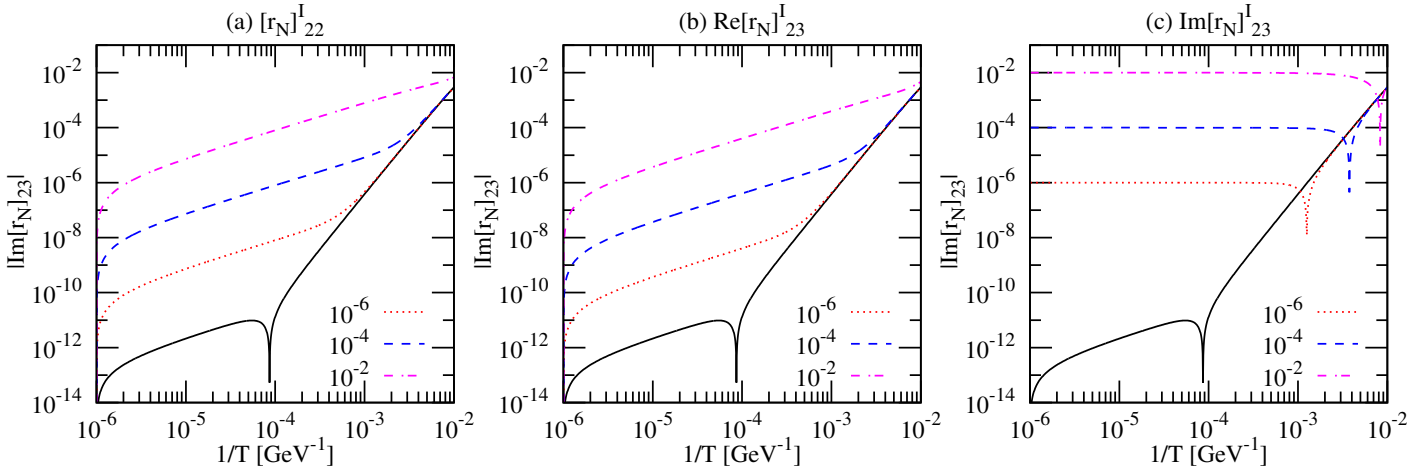

Figure 4: Evolution of $\mathrm{Im}[r_N]^I_{23}$ in the presence of the initial value of $[r_N]_{22}$ in the panel (a), $\mathrm{Re}[r_N]_{23}$ in the panel (b), and $\mathrm{Im}[r_N]_{23}$ in the panel (c). The initial value is taken as 0 (black solid line), 10^{-6} (red dotted line), 10^{-4} (blue dashed line), and 10^{-2} (magenda dot dashed line). We take here $\Delta M = 10^{-13}$ GeV, $X_\omega = 1$, $\omega_r = +0.909$, and $\eta = 2.15$.

We then discuss the impact of the initial value $\mathrm{Im}[r_N]^I_{23}$ in detail. We show in Fig. 5 the evolution of the elements of the matrix of densities in the presence of the nonzero $\mathrm{Im}[r_N]^I_{23}$. It is seen that the diagonal elements $[r_N]_{22}$ and $[r_N]_{33}$ do not change much by such an initial value. In addition, the real part of the off-diagonal element becomes modified only if $\mathrm{Im}[r_N]^I_{23}$ becomes sufficiently large as $\mathcal{O}(10^{-2})$. On the other hand, as shown in Fig. 5 (d), the initial value modifies drastically the initial evolution of $\mathrm{Im}[r_N]_{23}$, which leads to the change of the yield of the BAU.

Finally, we consider the cases when $X_\omega = 0.1$ and 0.01 where the overall scale of Yukawa coupling constants are enhanced by a factor 10 and 100 compared with the case $X_\omega = 1$ and then the strong washout of the BAU occurs. The deviations of the BAU for these cases are shown in Figs. 6 (a) and (b). It is interesting to note that the initial values of the matrices of densities give no impact on the yield of the BAU in these cases as long as they are smaller than $\mathcal{O}(10^{-2})$. This is expected since the information of the reheating epoch is lost due to the rapid thermalization processes. We also find by numerical calculations that this behavior does not change when the mass difference becomes smaller so that $T_{\rm osc} \ll T_{\rm sph}$ (which should be contrasted with the $X_\omega = 1$ case). Therefore, in the strong washout region the prediction of the BAU is insensitive to the initial values of the matrices of densities and the baryogenesis is just the low energy physics at $T \sim T_{\rm sph}$.

5 Conclusions

In this paper we have investigated the impacts of the higher dimensional operator (5) on the phenomenology of right-handed neutrinos in the νMSM. Especially, we have studied how the prediction of baryogenesis is altered by the initial abundance of right-handed neutrinos produced by the scatterings of Higgs bosons at the reheating epoch. We have parameterized such an abundance as the initial values

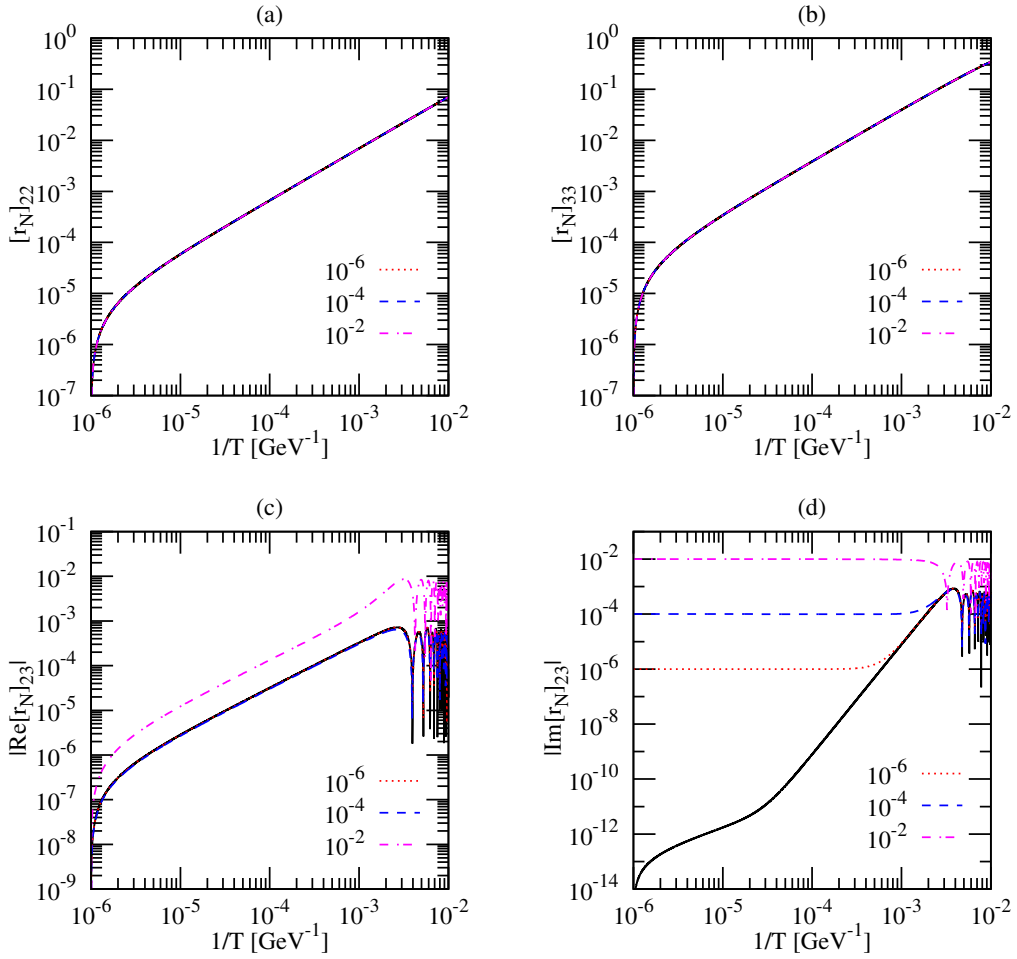

Figure 5: Evolution of element of the matrix of densities in the presence of the initial value of $\mathrm{Im}[r_N]^I_{23} = 0$ (black solid line), 10^{-2} (magenda dot dashed line), 10^{-4} (blue dashed line), and 10^{-6} (red dotted line). Evolution of $[r_N]_{22}$, $[r_N]_{33}$, $\mathrm{Re}[r_N]_{23}$, and $\mathrm{Im}[r_N]_{23}$ in the panels (a), (b), (c), and (d), respectively. We take here $\Delta M = 10^{-10}$ GeV, $X_\omega = 1$, $\omega_r = +0.01$, and $\eta = 2.15$.

of the matrices of densities $[r_N]^I_{IJ}$ and $[r_{\overline{N}}]^I_{IJ}$. Since the coupling matrix A in Eq. (5) is non-diagonal generally, the off-diagonal elements of $[r_N]^I_{IJ}$ and $[r_{\overline{N}}]^I_{IJ}$ can be present.

The initial abundance of N_1 at the reheating epoch may be responsible for the dark matter density of the present universe, and the viable parameter space of the N_1 mass and couplings is also enlarged. In such a case, right-handed neutrino N_1 can be dark matter even if its mass is much large than 10 keV scale, as long as the stability is ensured due to the discrete symmetry.

We have also discussed the impact on baryogenesis. It has been shown that the initial values do not change the yield of the BAU in the strong washout region as long as the overproduction of dark matter N_1 is avoided. Thus, in these cases the baryogenesis in the νMSM is insensitive to the physics at high energy scales such as the processes at the reheating epoch after the inflationary universe. In this case, the baryon asymmetry is a consequence of the mechanism at the weak scale physics. This strong washout region is very motivated since N_2 and N_3 are expected to be explored by future experiments as

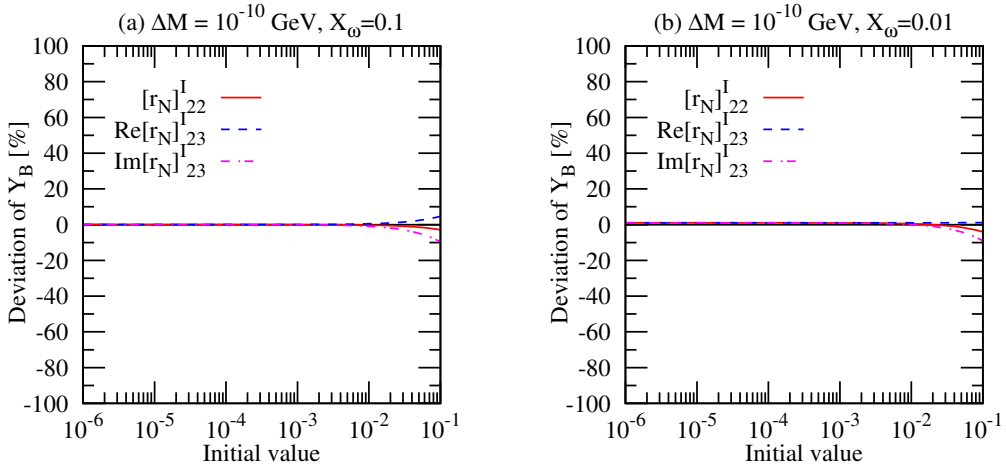

Figure 6: Same as Fig. 3 except for $\Delta M = 10^{-10}$ GeV and taken (a) $X_\omega = 0.1$ and (b) $X_\omega = 0.01$.

SHiP [49], LBNE (DUNE) [50], and FCC-ee [51] due to the larger mixing elements.

On the other hand, we have found the significant deviation due to the initial values in the weak washout region, which is contrasted to the previous study in Ref. [19]. When the oscillation effect is less important for baryogenesis ($T_{\rm osc} \ll T_{\rm sph}$), the initial values of all the components are important. On the other hand, when $T_{\rm osc} \gtrsim T_{\rm sph}$ and the baryogenesis is induced by the oscillation of N_2 and N_3, the initial values of the real and imaginary parts of the off-diagonal element are found to be significant. Under the choice of parameters in this analysis, any initial value smaller than $\mathcal{O}(10^{-5})$ is negligible for the prediction of the BAU. Such a small initial value can be obtained if the reheating temperature becomes smaller or the cutoff scale becomes higher. Otherwise, in the weak washout region the baryogenesis receives the influence of high energy physics. In some cases the generation of the BAU can be boosted and hence the region for the successful baryogenesis in the νMSM is enlarged.

We should stress that, although we have investigated the impact of the higher dimensional operator (5), our results can be applied to any mechanism giving the inital abundance of right-handed neutrinos at higher temperature region.

Acknowledgments

The work of T.A. was partially supported by JSPS KAKENHI Grant Numbers 15H01031 and 25400249. The work of S.E. was partially supported by the Swiss National Science Foundation 200020_162927/1. T.A., K.M., and T.Y. thank the Yukawa Institute for Theoretical Physics at Kyoto University, where this work was initiated during the YITP-S-16-04 on "the 21th Niigata-Yamagata joint school".

A Production of right-handed neutrinos

In this appendix we discuss the production of right-handed neutrinos by the operator (5). To make our argument clear, let us move to the basis in which the coupling matrix A is diagonal. This can be done by the unitary transformation as

$$\nu'_R = V_R \nu_R \,, \tag{25}$$

where the mixing matrix V_R is defined by the diagonalization of A as

$$V_R^* A V_R^\dagger = A' = \mathrm{diag}(A'_1, A'_2, A'_3) \,. \tag{26}$$

As we will see below, the production is most effective at the reheating epoch and the basis with ν'_R is more relevant to describe the production since the Majorana masses are negligible for $T_R \gg M_I$.

Let us then consider a pair production of ν'_{RI}:

$$\phi_a + \phi_a \to \nu'_{RI}(\vec{p}_1,\ h_1) + \nu'_{RI}(\vec{p}_2,\ h_2) \,. \tag{27}$$

where $\vec{p}_{1,2}$ and $h_{1,2}$ are three momenta and helicities of final particles, and four real scalar fields of the Higgs doublet Φ are denoted by ϕ_a ($a = 1,2,3,4$). The helicity amplitude is given by

$$M_{h_1,h_2} = \frac{1}{\Lambda} \bar{u}(\vec{p}_1, h_1) \left[A'_I P_R + A'^*_I P_L \right] v(\vec{p}_2, h_2) \,, \tag{28}$$

where $P_{L,R}$ are chiral projection operators $P_L = (1-\gamma_5)/2$ and $P_R = (1+\gamma_5)/2$. By neglecting the masses of right-handed neutrinos, we find the amplitudes in the center-of-mass frame are given by

$$M_{+-} = M_{-+} = 0 \,, \quad M_{++} = +\frac{\tilde{A}^*_I}{\Lambda} e^{-i\varphi_1} \sqrt{s} \,, \quad M_{--} = -\frac{\tilde{A}_I}{\Lambda} e^{+i\varphi_1} \sqrt{s} \,, \tag{29}$$

where $\vec{p}_1 = |\vec{p}_1|(\sin\theta_1 \cos\varphi_1,\ \sin\theta_1 \sin\varphi_1,\ \cos\theta_1)$ and $\sqrt{s}$ is the center-of-mass energy. It can be seen that the pair of the same helicity state is produced. The cross section of the process (27) is [19]

$$\sigma(\phi_a + \phi_a \to \nu'_{RI} + \nu'_{RI}) = \frac{|A'_I|^2}{16\Lambda^2} \,, \tag{30}$$

where the sum of helicities in the final state has been taken. Then, the scatterings of ϕ_a at reheating epoch generate ν'_{RI} and its yield for $T \ll T_R$ is given by [19]

$$\frac{n_{\nu'_{RI}} + n_{\overline{\nu'}_{RI}}}{s} = \frac{135\sqrt{10}\zeta^2(3)}{16\pi^8 g_*^{3/2}} \frac{|A'_I|^2 M_P\, T_R}{\Lambda^2} = 3.68 \times 10^{-6} \frac{|A'_I|^2 M_P\, T_R}{\Lambda^2} \,. \tag{31}$$

This leads to the matrices of densities for right-handed neutrinos and their antiparticles in the ν'_R basis as

$$[r_{N'}]_{IJ} = [r_{\overline{N'}}]_{IJ} = 9.44 \times 10^{-4} \frac{M_P\, T_R}{\Lambda^2} |A'_I|^2 \delta_{IJ} \,. \tag{32}$$

It is then found from (25) that the matrices of densities in the ν_R basis are given by

$$[r_N]_{IJ} = 9.44 \times 10^{-4} \frac{M_P\, T_R}{\Lambda^2} \left[A^\dagger A \right]_{IJ} \,, \quad [r_{\overline{N}}]_{IJ} = 9.44 \times 10^{-4} \frac{M_P\, T_R}{\Lambda^2} \left[A^T A^* \right]_{IJ} \,. \tag{33}$$

We can see that $r_N^\dagger = r_N$ and $r_{\overline{N}}^\dagger = r_{\overline{N}}$ as expected, and also that $r_{\overline{N}} = r_N^*$ which means that there is no asymmetry between ν_{RI} and $\overline{\nu}_{RI}$ induced by the process (27).

B Yukawa coupling constants of N_2 and N_3

In this appendix we show the parametrization of the Yukawa coupling constants of N_2 and N_3. We follow the notation in Ref. [48].

Without loss of generality we can parametrize $F_{\alpha I}$ ($I = 2,3$) as [52,53][#3]

$$F = \frac{i}{\langle\Phi\rangle} U D_\nu^{1/2} \Omega D_N^{1/2}. \tag{34}$$

Here $D_\nu = \mathrm{diag}(m_1, m_2, m_3)$ is the mass matrix of active neutrinos and the PMNS mixing matrix [20] is given by

$$U = \begin{pmatrix} c_{12}c_{13} & s_{12}c_{13} & s_{13}e^{-i\delta} \\ -c_{23}s_{12} - s_{23}c_{12}s_{13}e^{i\delta} & c_{23}c_{12} - s_{23}s_{12}s_{13}e^{i\delta} & s_{23}c_{13} \\ s_{23}s_{12} - c_{23}c_{12}s_{13}e^{i\delta} & -s_{23}c_{12} - c_{23}s_{12}s_{13}e^{i\delta} & c_{23}c_{13} \end{pmatrix} \times \mathrm{diag}(1,\ e^{i\eta},\ 1), \tag{35}$$

with $s_{ij} = \sin\theta_{ij}$ and $c_{ij} = \cos\theta_{ij}$. δ is a Dirac phase and η is a Majorana phase.

Throughout this work we consider the normal hierarchy of active neutrino masses:

$$m_3 > m_2 > m_1 = 0. \tag{36}$$

As for the mixing angles and mass squared differences, we use the central values in Ref. [54].

$$\begin{aligned} &\sin^2\theta_{12} = 0.306, && \sin^2\theta_{23} = 0.441, && \sin^2\theta_{13} = 0.02166, \\ &\Delta m^2_{21} = 7.50\times10^{-5}\ \mathrm{eV}^2, && \Delta m^2_{31} = 2.524\times10^{-3}\ \mathrm{eV}^2. \end{aligned} \tag{37}$$

$D_N = \mathrm{diag}(M_2, M_3)$ is the mass matrix of HNLs and we take $M_2 = M_N - \Delta M/2$ and $M_3 = M_N + \Delta M/2$. The 3×2 matrix Ω is given by

$$\Omega = \begin{pmatrix} 0 & 0 \\ \cos\omega & -\sin\omega \\ \xi\sin\omega & \xi\cos\omega \end{pmatrix}. \tag{38}$$

Here ω is a complex parameter and we parameterize its imaginary part as

$$X_\omega = \exp(\mathrm{Im}\omega), \tag{39}$$

and the real part is denoted as ω_r. Note that the physical region of these parameters is found, for example, in Ref. [55]. In the present analysis, we take the following values in all cases for simplicity.

$$M_N = 3\ \mathrm{GeV},\quad \xi = 1,\quad \delta = 1.45,\quad \eta = 2.15. \tag{40}$$

[#3] We set the coupling for dark matter N_1 as $F_{\alpha1} = 0$ for simplicity, since they are severely restricted by the cosmological constraints [27].

C Evolution of baryon asymmetry

In this appendix we shall show the evolution of the yield of the BAU depending on the non-zero initial value of the matrices of densities [56]. Note that the absolute value of Y_B is shown in the figures below and Y_B is negative in some regions. Here, Y_B is not the present value of the BAU but it is given by

$$Y_B(T) = 1.3 \times 10^{-3} \sum_{\alpha} \mu_{B/3-L_\alpha}(T)\,, \tag{41}$$

until $T = 100$ GeV, which should not be confused with Y_B in Eq. (22).

C.1 Weak washout regime

First of all, we consider the region in which the Yukawa coupling constants are so small that the washout process of the asymmetries is ineffective.

C.1.1 The case with $T_{\rm osc} \ll T_{\rm sph}$

We take the following parameter set.

$$M_N = 3\ \text{GeV}, \quad \Delta M = 10^{-13}\ \text{GeV}, \quad X_\omega = 1, \quad \omega_r = +0.909, \quad \delta = 1.45, \quad \eta = 2.15, \tag{42}$$

which correspond to the case Fig. 3 (a). The evolution of $|Y_B|$ is shown in Fig. 7.

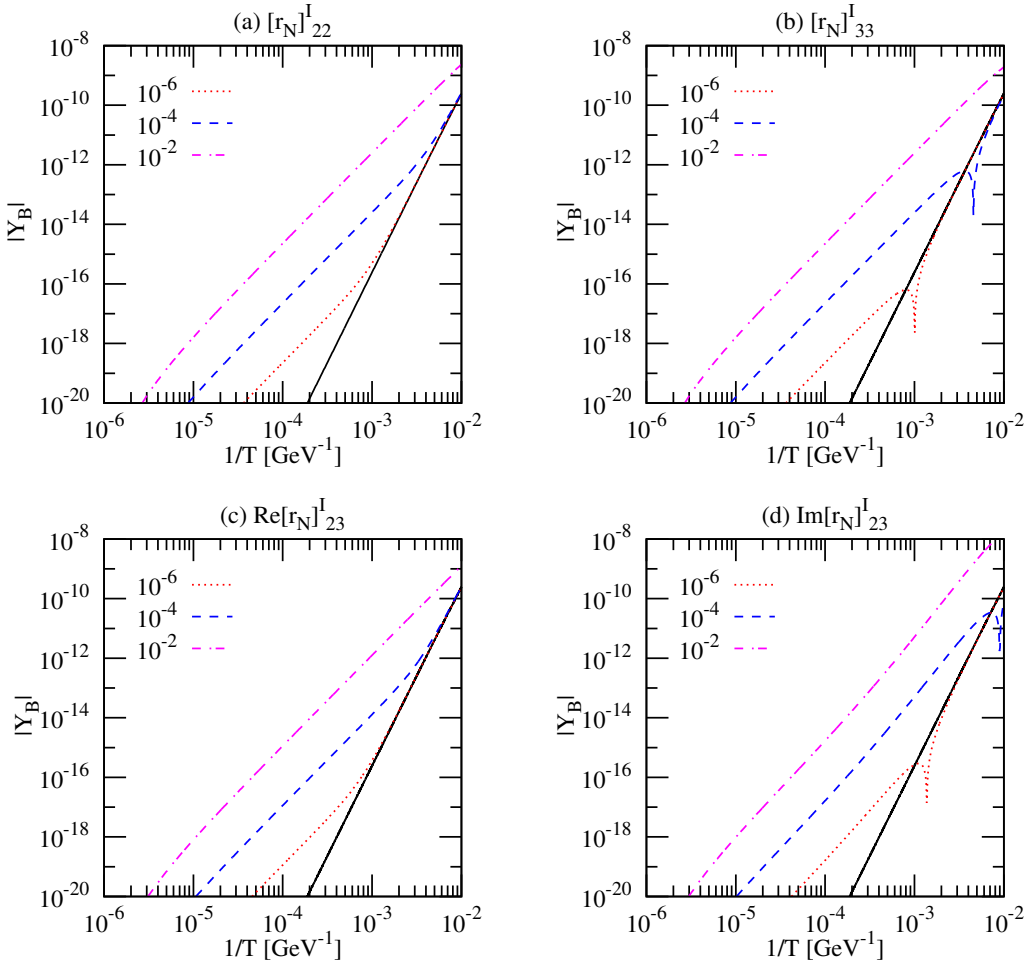

Figure 7: Evolution of the BAU when $\Delta M = 10^{-13}$ GeV and $X_\omega = 1$. Black solid line shows the BAU when there is no initial value for all the elements of the matrix of densities. The red dotted, blue dashed, and magenta dot dashed lines correspond to the cases where the initial value of the element is 10^{-2}, 10^{-4}, and 10^{-6}. The non-zero initial value is given for $[r_N]_{22}$, $[r_N]_{33}$, $\mathrm{Re}[\mathrm{r_N}]_{23}$, and $\mathrm{Im}[\mathrm{r_N}]_{23}$ at the panels (a), (b), (c), and (d).

C.1.2 The case with $T_{\rm osc} \sim T_{\rm sph}$

We take the following parameter set.

$$M_N = 3\ \text{GeV}, \quad \Delta M = 10^{-10}\ \text{GeV}, \quad X_\omega = 1, \quad \omega_r = +0.01, \quad \delta = 1.45, \quad \eta = 2.15, \tag{43}$$

which correspond to the case Fig. 3 (b). The evolution of $|Y_B|$ is shown in Fig. 8.

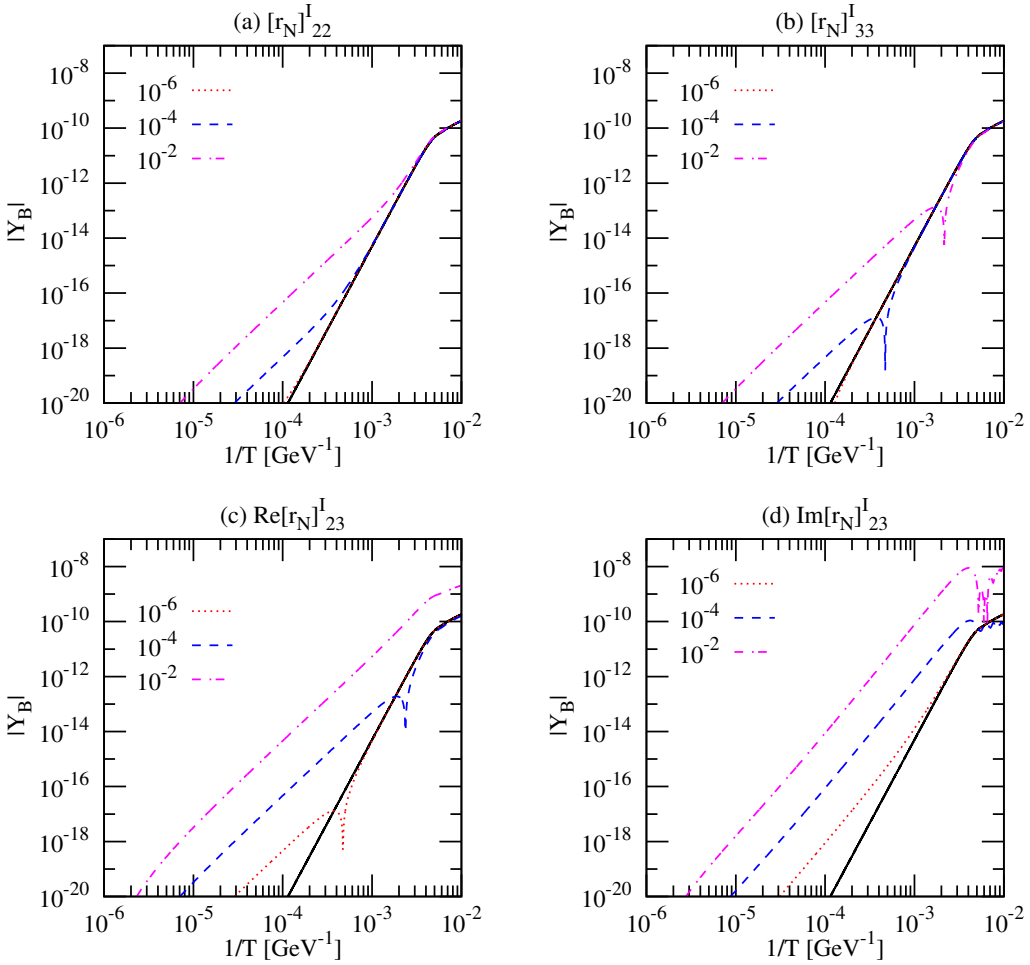

Figure 8: Same as Fig. 5 except for $\Delta M = 10^{-10}$ GeV and $X_\omega = 1$.

C.1.3 The case with $T_{\rm osc} \gg T_{\rm sph}$

We take the following parameter set.

$$M_N = 3\ \text{GeV}, \quad \Delta M = 10^{-7}\ \text{GeV}, \quad X_\omega = 1, \quad \omega_r = +0.909, \quad \delta = 1.45, \quad \eta = 2.15, \tag{44}$$

which correspond to the case Fig. 3 (c). The evolution of $|Y_B|$ is shown in Fig. 9.

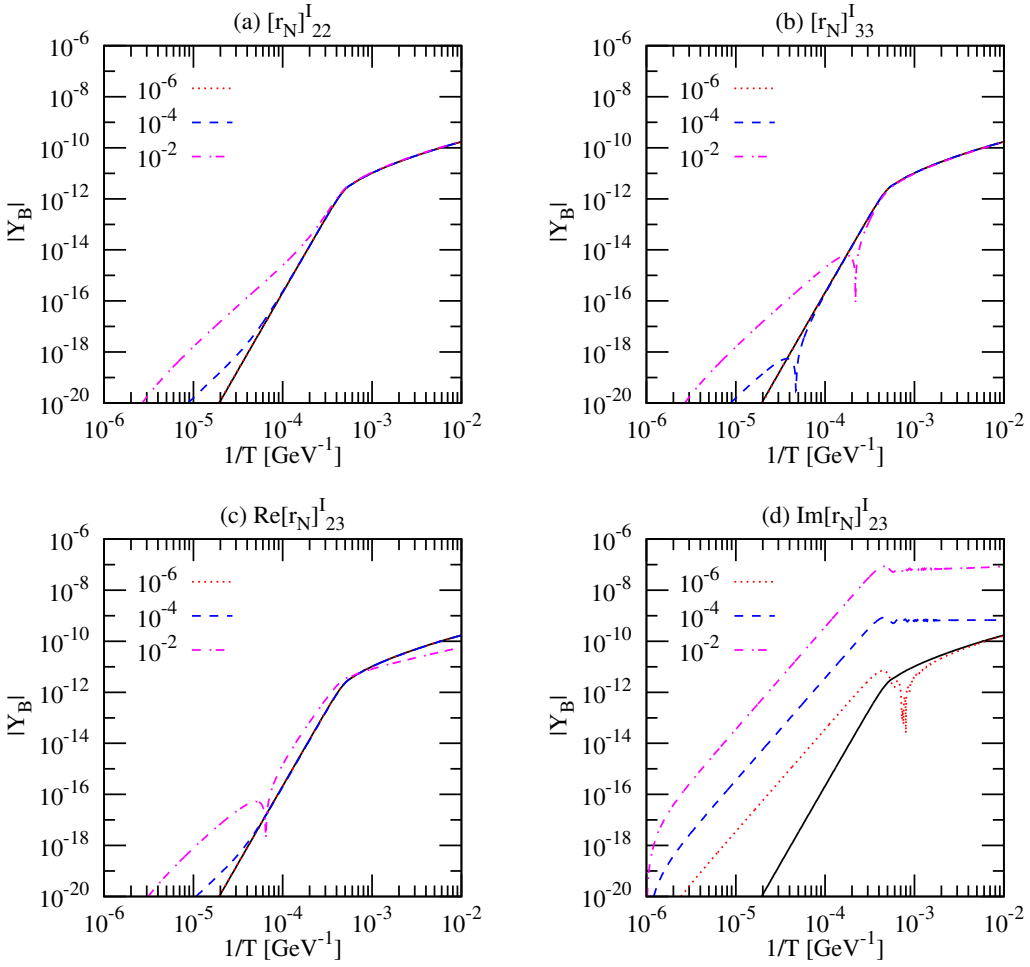

Figure 9: Same as Fig. 5 except for $\Delta M = 10^{-7}$ GeV and $X_\omega = 1$.

C.2 Strong washout regime

Next, we turn to consider the region in which the Yukawa coupling constants are so large that the strong washout of the asymmetries takes place.

C.2.1 The case with $T_{\rm osc} \sim T_{\rm sph}$ and $X_\omega = 0.1$

We take the following parameter set.

$$M_N = 3\ \text{GeV}, \quad \Delta M = 10^{-10}\ \text{GeV}, \quad X_\omega = 0.1, \quad \omega_r = +0.909, \quad \delta = 1.45, \quad \eta = 2.15, \tag{45}$$

which correspond to the case Fig. 6 (a). The evolution of $|Y_B|$ is shown in Fig. 10.

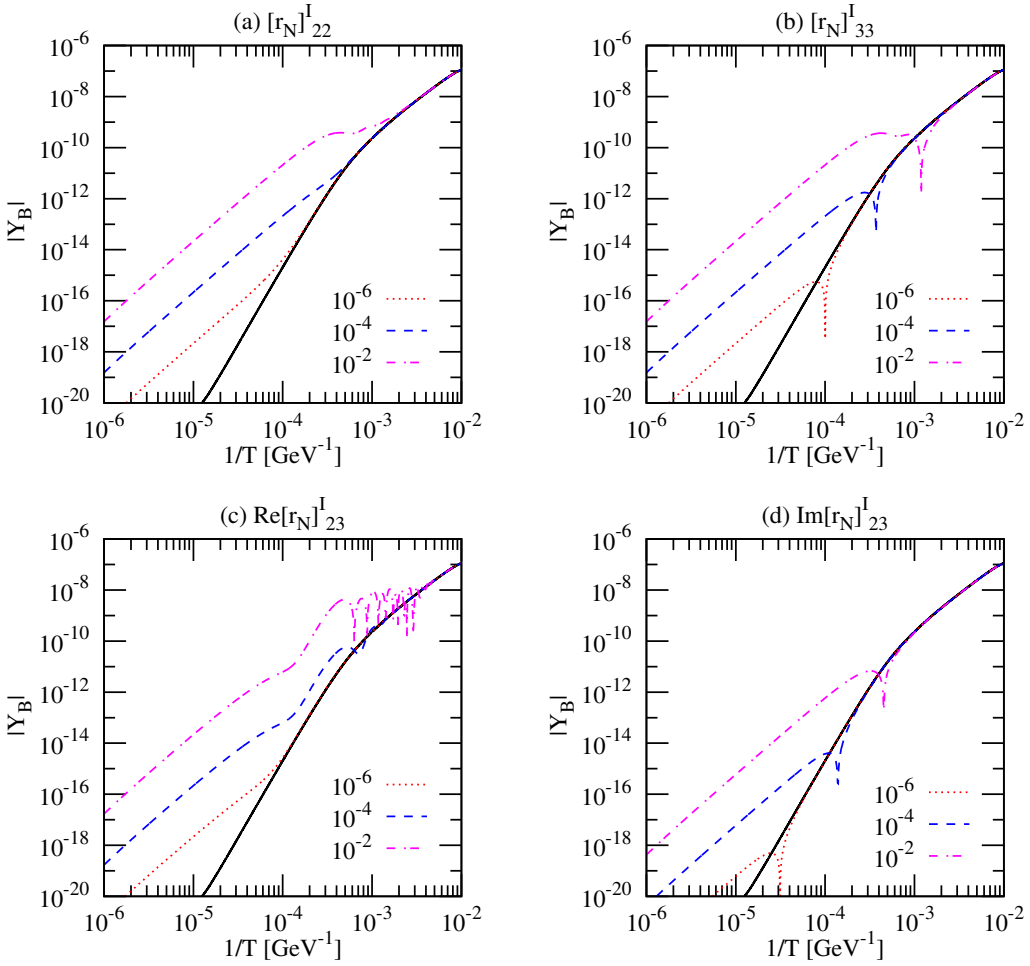

Figure 10: Same as Fig. 5 except for $\Delta M = 10^{-10}$ GeV and $X_\omega = 0.1$.

C.2.2 The case with $T_{\rm osc} \sim T_{\rm sph}$ and $X_\omega = 0.01$

We take the following parameter set.

$$M_N = 3\ \text{GeV}, \quad \Delta M = 10^{-10}\ \text{GeV}, \quad X_\omega = 0.01, \quad \omega_r = +0.909, \quad \delta = 1.45, \quad \eta = 2.15, \tag{46}$$

which correspond to the case Fig. 6 (b). The evolution of $|Y_B|$ is shown in Fig. 11.

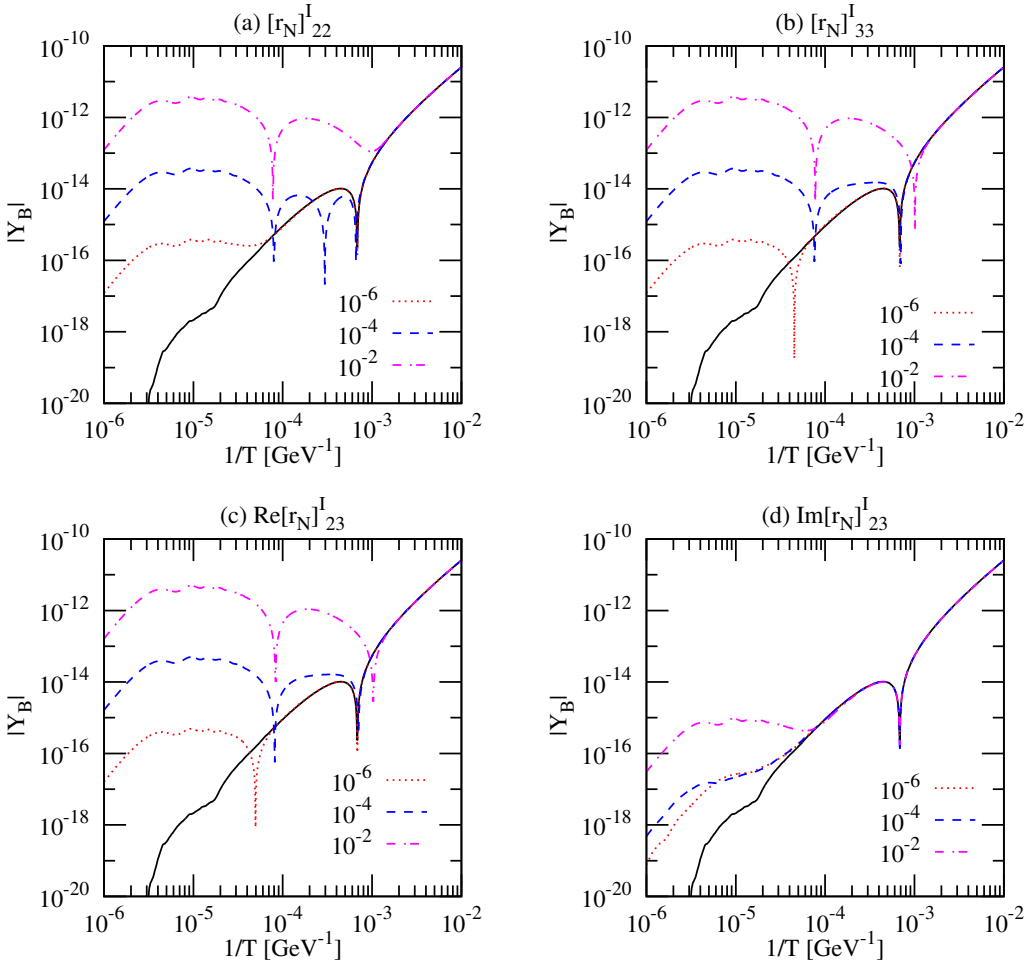

Figure 11: Same as Fig. 5 except for $\Delta M = 10^{-10}$ GeV and $X_\omega = 0.01$.

References

[1] P. A. R. Ade *et al.* [Planck Collaboration], Astron. Astrophys. **594** (2016) A13 [arXiv:1502.01589 [astro-ph.CO]].

[2] A. D. Sakharov, Pisma Zh. Eksp. Teor. Fiz. **5** (1967) 32 [JETP Lett. **5** (1967) 24] [Sov. Phys. Usp. **34** (1991) 392] [Usp. Fiz. Nauk **161** (1991) 61].

[3] M. D'Onofrio and K. Rummukainen, Phys. Rev. D **93** (2016) no.2, 025003 [arXiv:1508.07161 [hep-ph]].

[4] P. Minkowski, Phys. Lett. B **67**, 421 (1977).

[5] T. Yanagida, in Proceedings of the Workshop on Unified Theory and Baryon Number of the Universe, edited by.O. Sawada and A. Sugamoto (KEK, Tsukuba, Ibaraki 305- 0801 Japan, 1979) p. 95.

[6] T. Yanagida, Prog. Theor. Phys. **64**, 1103 (1980).

[7] M. Gell-Mann, P. Ramond, and R. Slansky, in Supergravity, edited by.P. van Niewwenhuizen and D. Freedman (North Holland, Amsterdam, 1979) [arXiv:1306.4669 [hep-th]].

[8] P. Ramond, in *Talk given at the Sanibel Symposium*, Palm Coast, Fla., Feb. 25-Mar. 2, 1979, preprint CALT-68-709 (retroprinted as hep-ph/9809459).

[9] S. L. Glashow, in *Proc. of the Cargése Summer Institute on Quarks and Leptons*, Cargése, July 9-29, 1979, eds. M. Lévy et. al, , (Plenum, 1980, New York), p707.

[10] R. N. Mohapatra and G. Senjanovic, Phys. Rev. Lett. **44** (1980) 912.

[11] M. Fukugita and T. Yanagida, Phys. Lett. B **174** (1986) 45 .

[12] V. A. Kuzmin, V. A. Rubakov and M. E. Shaposhnikov, Phys. Lett. **155B** (1985) 36.

[13] G. F. Giudice, A. Notari, M. Raidal, A. Riotto and A. Strumia, Nucl. Phys. B **685** (2004) 89 [arXiv:hep-ph/0310123].

[14] W. Buchmuller, R. D. Peccei and T. Yanagida, Ann. Rev. Nucl. Part. Sci. **55** (2005) 311 [arXiv:hep-ph/0502169];

[15] S. Davidson, E. Nardi and Y. Nir, Phys. Rept. **466**, 105 (2008) [arXiv:0802.2962 [hep-ph]].

[16] E. K. Akhmedov, V. A. Rubakov and A. Y. Smirnov, Phys. Rev. Lett. **81** (1998) 1359.

[17] T. Asaka and M. Shaposhnikov, Phys. Lett. B **620**, 17 (2005) [hep-ph/0505013].

[18] T. Asaka, S. Blanchet and M. Shaposhnikov, Phys. Lett. B **631** (2005) 151 [hep-ph/0503065].

[19] F. Bezrukov, D. Gorbunov and M. Shaposhnikov, JCAP **0906** (2009) 029 [arXiv:0812.3622 [hep-ph]].

[20] B. Pontecorvo, Sov. Phys. JETP **7** (1958) 172;
Z. Maki, M. Nakagawa and S. Sakata, Prog. Theor. Phys. **28** (1962) 870.

[21] A. Boyarsky, A. Neronov, O. Ruchayskiy, M. Shaposhnikov and I. Tkachev, Phys. Rev. Lett. **97** (2006) 261302 [astro-ph/0603660].

[22] S. Dodelson and L. M. Widrow, Phys. Rev. Lett. **72**, 17 (1994) [hep-ph/9303287].

[23] A. Boyarsky, J. Lesgourgues, O. Ruchayskiy and M. Viel, JCAP **0905** (2009) 012 [arXiv:0812.0010 [astro-ph]].

[24] X. D. Shi and G. M. Fuller, Phys. Rev. Lett. **82** (1999) 2832 [astro-ph/9810076].

[25] T. Asaka, M. Laine and M. Shaposhnikov, JHEP **0701** (2007) 091 Erratum: [JHEP **1502** (2015) 028] [hep-ph/0612182].

[26] A. Boyarsky, O. Ruchayskiy and M. Shaposhnikov, Ann. Rev. Nucl. Part. Sci. **59** (2009) 191 [arXiv:0901.0011 [hep-ph]].

[27] M. Drewes *et al.*, JCAP **1701** (2017) no.01, 025 [arXiv:1602.04816 [hep-ph]].

[28] M. Laine and M. Shaposhnikov, JCAP **0806** (2008) 031 [arXiv:0804.4543 [hep-ph]].

[29] L. Canetti, M. Drewes and M. Shaposhnikov, Phys. Rev. Lett. **110**, no. 6, 061801 (2013) [arXiv:1204.3902 [hep-ph]].

[30] L. Canetti, M. Drewes, T. Frossard and M. Shaposhnikov, Phys. Rev. D **87**, 093006 (2013) [arXiv:1208.4607 [hep-ph]].

[31] S. Mertens, K. Dolde, M. Korzeczek, F. Glueck, S. Groh, R. D. Martin, A. W. P. Poon and M. Steidl, Phys. Rev. D **91** (2015) 042005 [arXiv:1410.7684 [hep-ph]].

[32] S. Mertens *et al.*, JCAP **1502** (2015) no.02, 020 [arXiv:1409.0920 [physics.ins-det]].

[33] T. Asaka, S. Eijima and H. Ishida, JCAP **1202** (2012) 021 [arXiv:1112.5565 [hep-ph]].

[34] L. Canetti, M. Drewes and B. Garbrecht, Phys. Rev. D **90**, no. 12, 125005 (2014) [arXiv:1404.7114 [hep-ph]].

[35] M. Shaposhnikov, JHEP **0808** (2008) 008 [arXiv:0804.4542 [hep-ph]].

[36] L. Canetti and M. Shaposhnikov, JCAP **1009** (2010) 001 [arXiv:1006.0133 [hep-ph]].

[37] V. V. Khoze and G. Ro, JHEP **1310** (2013) 075 [arXiv:1307.3764 [hep-ph]].

[38] B. Shuve and I. Yavin, Phys. Rev. D **89** (2014) no.7, 075014 [arXiv:1401.2459 [hep-ph]].

[39] B. Garbrecht, Phys. Rev. D **90** (2014) no.6, 063522 [arXiv:1401.3278 [hep-ph]].

[40] A. Abada, G. Arcadi, V. Domcke and M. Lucente, JCAP **1511** (2015) no.11, 041 [arXiv:1507.06215 [hep-ph]].

[41] P. Hernández, M. Kekic, J. López-Pavón, J. Racker and N. Rius, JHEP **1510** (2015) 067 [arXiv:1508.03676 [hep-ph]].

[42] A. Kartavtsev, P. Millington and H. Vogel, JHEP **1606** (2016) 066 [arXiv:1601.03086 [hep-ph]].

[43] M. Drewes, B. Garbrecht, D. Gueter and J. Klaric, JHEP **1612** (2016) 150 [arXiv:1606.06690 [hep-ph]].

[44] P. Hernández, M. Kekic, J. López-Pavón, J. Racker and J. Salvado, JHEP **1608** (2016) 157 [arXiv:1606.06719 [hep-ph]].

[45] I. Ghisoiu and M. Laine, JCAP **1412** (2014) no.12, 032 [arXiv:1411.1765 [hep-ph]].

[46] D. Buttazzo, G. Degrassi, P. P. Giardino, G. F. Giudice, F. Sala, A. Salvio and A. Strumia, JHEP **1312** (2013) 089 [arXiv:1307.3536 [hep-ph]].

[47] M. D'Onofrio, K. Rummukainen and A. Tranberg, Phys. Rev. Lett. **113** (2014) no.14, 141602 [arXiv:1404.3565 [hep-ph]].

[48] T. Asaka, S. Eijima and H. Ishida, JHEP **1104** (2011) 011 [arXiv:1101.1382 [hep-ph]].

[49] M. Anelli *et al.* [SHiP Collaboration], arXiv:1504.04956 [physics.ins-det].

[50] C. Adams *et al.* [LBNE Collaboration], arXiv:1307.7335 [hep-ex].

[51] A. Blondel *et al.* [FCC-ee study Team Collaboration], arXiv:1411.5230 [hep-ex].

[52] J. A. Casas and A. Ibarra, Nucl. Phys. B **618** (2001) 171 [arXiv:hep-ph/0103065].

[53] A. Abada, S. Davidson, A. Ibarra, F. X. Josse-Michaux, M. Losada and A. Riotto, JHEP **0609** (2006) 010 [arXiv:hep-ph/0605281].

[54] I. Esteban, M. C. Gonzalez-Garcia, M. Maltoni, I. Martinez-Soler and T. Schwetz, JHEP **1701** (2017) 087 [arXiv:1611.01514 [hep-ph]].

[55] T. Asaka, S. Eijima, H. Ishida, K. Minogawa and T. Yoshii, in preparation.

[56] K. Minogawa, Master Thesis (2017).